

Temperature and radon-222 as tracer of groundwater flow: application to El Hamma geothermal aquifer system, southeastern Tunisia

Agoubi Belgacem¹ · Faiza Souid¹ · Faten Telahigue¹ · Adel Kharroubi¹

Received: 21 November 2014 / Accepted: 15 June 2015 / Published online: 27 June 2015
© Saudi Society for Geosciences 2015

Abstract Hydrogeological and hydrochemical investigations were applied to explain geothermal groundwater flow factors controlling groundwater mineralization, and ²²²Rn concentrations were controlled using RAD7-H₂O in El Hamma aquifer system, southeastern Tunisia. Nineteen geothermal water samples were collected from different locations (thermal baths and deep wells). Physical parameters (EC, pH, TDS, T) were measured, and major ions were analyzed. Hydrogeochemical modeling and thermal parameters reveal that groundwater from El Hamma aquifer system has several origins. The first type was characterized by a hot temperature >55 °C with a chemical facies Na-Mg-Ca-SO₄-Cl. This type characterizes lower cretaceous deep water (continental intercalary aquifer). The second water type was dominated by Na-Ca-Cl-SO₄ facies with a temperature <45 °C and represents the superficial aquifer. However, Ca-SO₄-Na-Cl-Mg is the third water type which is characterized by mixed water from deep and shallow water with a temperature ranging from 45 to 55 °C. Shallow aquifer displays higher ²²²Rn concentration (677 to 2903 Bq/m³). However, deep water from continental intercalary displays relatively a low radon concentration (203 to 1100 Bq/

m³). Compared to Rn-222 activity in some countries, radon concentration in El Hamma thermal aquifer system has a medium value controlled by structures, porosity, and permeability of aquifers. Variographic analysis and ordinary kriging techniques were used to map temperature spatial variability in the study area. Geostatistical techniques in addition to geological data and radon activities confirm the existence of vertical communication between continental intercalary aquifer and superficial Senonian aquifer through vertical faults system.

Keywords Geochemical · Radon-222 · Geothermal aquifer · El hamma · Tunisia

Introduction

Located in southeast of Tunisia, El Hamma City was recognized as a thermal spring since the Roman times. It was long the destination of thousands of people from Tunisia and neighboring countries for care and bathing. Since 1980, El Hamma region recognized an implementation of irrigated areas and wide areas of geothermal greenhouses which has made the region an international geothermal site. The industry is also a potential consumer of El Hamma groundwater aquifer. In recent decades, this region recognizes an imbalance of their ecosystems expressed as a qualitative and quantitative deterioration of groundwater resources and a rapid decrease of water table due to excessive pumping to satisfy agricultural, industrial, and domestic needs.

The thermal groundwater is generally accompanied by intense radon activities. Thermal springs are generally privileged places of radon emanation (King et al. 1996; Jalili-Majarehshin et al. 2012). It was recognized that high concentrations of radon in water may pose a serious health threat

Groundwater samples were collected, in December 2013, from 19 different locations (thermal baths and deep wells).

✉ Agoubi Belgacem
belgacem.agoubi@isstegb.mu.tn

Faiza Souid
faizasouid@yahoo.fr

Faten Telahigue
faten_telahigue@yahoo.fr

Adel Kharroubi
Adel.Kharroubi@isstegb.rnu.tn

¹ Higher Institute of Water Sciences and Techniques, University of Gabes, Campus universitaire, 6033 Gabes, Tunisia

to humans as radon-222 (^{222}Rn) is a known carcinogen (USEPA 1999). Radon is the number one cause of lung cancer among nonsmokers; overall, radon is the second leading cause of lung cancer and is responsible for some thousand cancer deaths every year (USEPA 2008).

^{222}Rn is a naturally occurring radionuclide; it is a gas which is formed by a series radioactive decay of uranium-238 (^{238}U). Radium 226 (^{226}Ra) is the parent radionuclide of ^{222}Rn in the decay series, and ^{226}Ra is found in a wide variety of rocks and soils (Gokhale and Leung 2010). The isotope ^{222}Rn has a half-life of 3.83 days and can therefore accumulate in the atmosphere and natural waters (Kendall and McDonnell 1998; Wu et al. 2003).

Radon is the most significant natural source of human radiation exposure. Radon is present in soil, rocks, building materials, and waters (King et al. 1996; Senior 1998; Kendall and McDonnell 1998; Wu et al. 2003; Voronov 2004; Gokhale and Leung 2010). Through diffusion and convection, radon migrates and emanates to the atmosphere. Its concentration in groundwater varies because of variable concentrations of sources in the aquifer materials, emanation rates from mineral sources, aquifer porosity, and permeability. It constitutes the major part of the radioactive gases present in mineral and groundwater (Nikolopoulos et al. 2009; Jalili-Majareshin et al. 2012).

Numerous factors such as geology, geochemical properties of parent radionuclides, hydrogeological conditions, abundance of parent radionuclides, and radionuclides sorbed by the rocks or soils are potential parameters that can affect ^{222}Rn groundwater concentration (Gokhale and Leung 2010). Radon can migrate away from its source in rock materials because of differences in physical and chemical properties. Previous studies have indicated that ^{222}Rn concentration in groundwater was due to passing through rocks and sediments of different compositions, mineral waters contain different salts of radium and thorium, which are subsequently decayed to radon (Kendall and McDonnell 1998; Wu et al. 2003). However, because of the short half-life of thoron, radon constitutes the major part of the radioactive gases present in mineral and groundwater (Jalili-Majareshin et al. 2012). Gurler et al. (2010) indicate that the radon concentration in Bursa in Turkey was due to mixed water in some baths from outside sources with very low radon concentration. King et al. (1996) published the spatial distribution of elevated ^{222}Rn concentrations in groundwater is described and related to factors that include sources within the aquifer, lithology, aquifer and well-construction characteristics, groundwater chemistry, and hydrogeologic setting (Senior 1998). Akawwi (2014) indicates a significant correlation between radon concentration and water temperature and a negative correlation between salt and radon concentration.

The main sources of radon in groundwater are rocks. All rocks contain some uranium, although most of them contain

very small amounts—between 1 and 3 ppm (Voronov 2004). Other sources of radon in groundwater are secondary deposits of radium salts. Most of the radon produced within a mineral grain remains embedded in the grain, and 10–50 % escapes to enter the pore space. This value is called the emanation coefficient. It is a ratio of emitted and original radon.

The emanation coefficient depends on the type of rock and its structure and porosity. Because of the presence of water in the pore space, the radon atoms can dissolve in groundwater. Therefore, first of all, the radon concentration in groundwater depends on the radioactivity of rocks and the emanation coefficient (Voronov 2004). Different concentrations of radon in water are due to different geological and hydrogeological conditions. Some areas in the world have exceptionally high concentrations of radon, such as, Brazil, India, Iran, and Canada. There are many springs with high levels of radon in Iran. In Scandinavia, there are high regional levels of radon (Voronov 2004; Jalili-Majareshin et al. 2012).

In the literature, several works are published on the use of temperature as a tracer of groundwater flow (Bravo et al. 2002; Stonestrom and Constantz 2003; Becker et al. 2004; El-Fiky 2009). Groundwater temperature can be measured easily and rapidly by lowering a thermometer down a borehole, although precautions must be taken to ensure that the recorded temperature is representative of water in the aquifer and not influenced by movement of water in the borehole (El-Fiky 2009). Temperature measurement in the borehole is inexpensive and widely available to detect areas of ground water discharge (Becker et al. 2004).

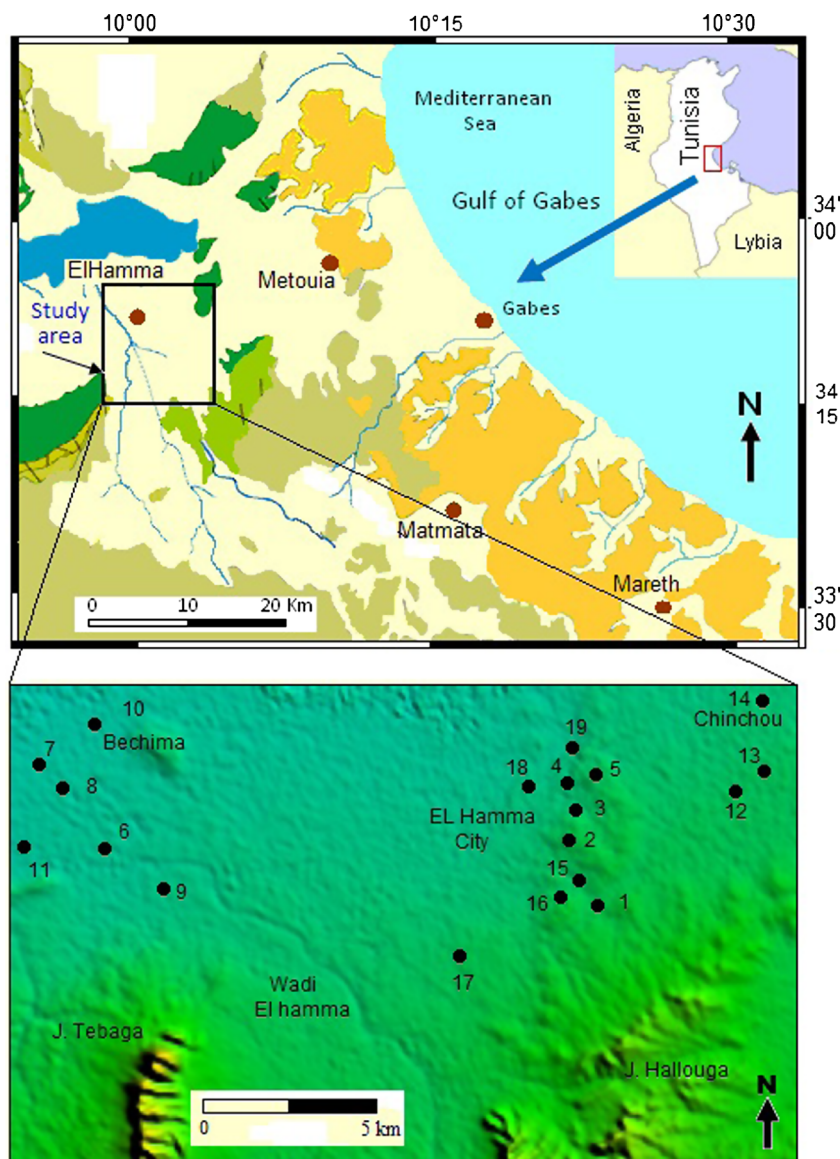
The purpose of this paper is to use combined geothermal groundwater chemistry, temperature, and radon activities as tracer to understand geothermal groundwater flow of El Hamma aquifer system. The second objective is to study radon concentration in thermal groundwater and understand the main factors controlling ^{222}Rn activity through a conceptual model of radon emanation. For this purpose, multidisciplinary approaches, that is, hydrogeochemical, statistical analysis, kriging techniques, hydrodynamic and modeling tools have been used. A regional hydrochemical survey was performed, and an integrated interpretation of acquired hydrochemical datasets was considered.

Material and methods

Study area description

This study has been carried out in El Hamma region, south-eastern Tunisia (Fig. 1). This region is underlain by Quaternary, Neogene, and Cretaceous rock units (Louhaichi and Tlig 1993). Upper Cretaceous is represented by the Cenomanian, Turonian, and lower Senonian. Mio-Pliocene, formed by

Fig. 1 Location and geologic map of the study area with inventory of water samples point (well and thermal bath)



gypseous marls, red marls and clays, conglomerates, pebbles, and sands (Ben Ouezdou 1984). A faults system has affected El Hamma region which induced a distinct lateral compartmentalization. All water-bearing formations of the study area are hydraulically connected through the vertical faults system.

The Senonian formation formed by marl and gypsum is surmounted by a limestone with a thickness ranging from 50 to 500 m (Castany 1982). These formations are strongly

fissured and constitute an important aquifer characterized by high transmissivity. The continental lower Cretaceous formations, formed by a complex succession of clastic sediments, contain a Continental Intercalary (CI) aquifer. Thickness and lithology of these layers reveal significant lateral variation (Edmunds et al. 2003). The CI aquifer system shows hydraulic continuity across northwestern Sahara (Castany 1982). El Hamma aquifer system is transacted by a network of

Table 1 Chemical analysis of sampled waters from the study area

ID no.	EC à 25 °C (ms/cm)	T (°C)	TDS (mg/l)	pH	Major ions (mg/l)										
					HCO ₃ ⁻	F ⁻	Cl ⁻	Br ⁻	NO ₃ ⁻	SO ₄ ²⁻	Li ⁺	Na ⁺	K ⁺	Ca ²⁺	Mg ²⁺
1	4.520	43.000	2523.157	7.080	261.130	3.231	761.846	2.194	3.114	676.264	0.375	396.283	13.617	446.197	111.383
2	4.550	44.000	2561.481	6.830	283.080	3.217	796.620	2.414	2.547	608.809	0.535	411.417	21.722	470.536	105.230
3	4.270	43.000	2318.457	7.140	266.130	3.479	663.952	1.165	3.461	652.381	1.810	334.585	22.456	429.920	118.243
4	4.830	38.500	2711.817	7.230	261.230	2.206	872.326	6.565	0.439	690.256	2.017	468.061	12.169	412.196	123.972
5	4.620	43.000	2561.927	7.380	272.180	2.558	738.643	6.066	0.926	720.547	1.921	409.591	19.147	418.550	107.671
6	4.430	45.000	2418.371	7.490	263.220	3.219	643.357	5.518	3.179	700.406	1.924	332.384	99.464	400.168	114.962
7	5.780	65.000	3291.851	8.010	271.220	0.676	956.044	2.953	38.976	983.475	0.386	622.615	16.574	418.264	135.131
8	4.810	64.800	2637.194	7.620	283.110	2.271	732.955	1.634	18.758	905.037	0.424	344.056	14.146	406.133	131.810
9	4.630	62.000	2588.346	7.130	269.230	3.164	744.322	1.630	15.160	854.412	0.443	327.290	17.245	392.791	138.429
10	4.610	39.000	2573.628	7.310	273.230	1.901	771.137	1.701	42.672	703.453	0.424	363.028	14.083	445.630	116.349
11	4.780	60.000	2661.594	7.710	279.330	2.555	695.776	2.100	61.513	877.558	0.448	333.958	15.858	400.918	153.214
12	5.160	46.000	2842.168	8.020	278.240	3.017	852.416	3.053	3.742	837.879	0.661	412.233	20.789	448.951	153.983
13	3.980	48.000	2173.691	7.420	274.540	3.115	443.801	1.624	67.132	780.663	0.428	211.745	15.662	410.216	129.940
14	4.120	30.000	2332.056	7.390	278.310	1.692	527.929	1.742	47.770	799.418	0.405	268.865	14.796	418.756	139.928
15	3.770	46.400	2118.308	8.110	286.430	2.219	472.718	1.658	36.559	746.311	0.416	204.069	14.450	386.141	134.506
16	3.730	51.100	2192.517	8.020	283.230	2.180	435.906	1.717	33.577	772.534	0.434	206.339	14.797	376.201	132.449
17	4.010	45.000	2163.519	7.220	279.440	3.162	461.724	2.184	18.950	743.683	0.451	215.553	15.946	471.951	111.543
18	4.230	38.000	2511.307	7.310	284.170	2.521	678.115	3.052	74.226	710.372	0.525	421.560	15.660	372.315	122.393
19	4.250	38.500	2443.511	7.620	284.340	3.541	618.808	2.250	19.544	792.530	0.846	344.828	16.077	411.875	128.998

reactivated and perennial faults and emerges through a line of springs which follows the wadi El Hamma and a high temperature gradient (45–70 °C) (Edmunds et al. 2003).

Sampling and analytical methods

Groundwater samples were collected, in December 2013, from 19 different locations (thermal baths and deep

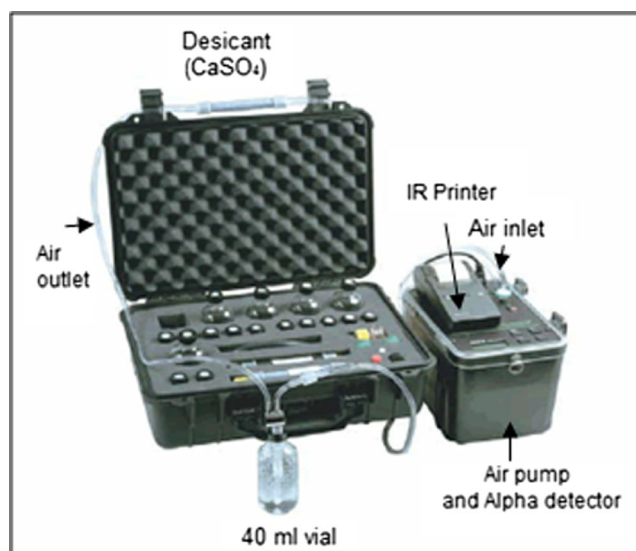


Fig. 2 RAD7 H₂O circuit with a 40-ml vial (Durrige Company Inc. 2000)

wells). Geographic coordinates (latitude, longitude, altitude) were measured using Trimble GPS. Total dissolved solids (TDS), electrical conductivity (EC), and potential hydrogen (pH) were measured in the field using a multi-parameter C933 Multi-Parameter analyzer (Table 1). Major ions (Na, K, Ca, Mg, F, NO₃, Cl, SO₄, and HCO₃) were analyzed using ionic chromatography (Methrohm 850 Professional IC) in the laboratory of geochemical analysis of Higher Institute of Water Sciences and Techniques, University of Gabes.

All the radon concentration measurements were carried out with alpha detector electronic radon detector RAD7 (Fig. 2). All groundwater radon measurements were carried out accordingly to instructions use of RAD7 H₂O. The RAD7 (H₂O) method (Durrige Company Inc. 2000) was used with eight 40-mL vials, which were rinsed in the water of the corresponding spring and dried completely prior to sample collection. For each location, three measurements were taken and then averaged.

Results and discussion

Hydrogeochemistry

The chemical composition of groundwater from El Hamma geothermal aquifer has been the subject of several investigations (Bouri et al. 2008; Trabelsi et al. 2009; Sahli et al. 2013;

Table 2 Basic statistics of physical parameters and major ions

	Unit	Min	Max	Mean	SD	Kurtosis	Skewness
T	°C	43.000	65.000	50.750	8.530	-1.340	0.690
pH		6.830	8.110	5.980	0.360	-0.660	0.380
EC	ms/cm	3.730	5.780	4.480	0.490	1.470	0.810
TDS	g/l	2.120	3.290	2.500	0.280	1.990	1.040
HCO ₃	mg/l	261.000	286.000	275.400	8.200	-1.000	-0.500
F	mg/l	0.700	3.500	2.600	0.700	1.300	-1.000
Cl	mg/l	435.900	956.000	677.300	152.100	-0.700	-0.300
NO ₃	mg/l	0.400	74.200	25.900	24.200	-0.700	0.700
SO ₄	mg/l	608.800	983.500	766.100	94.200	0.300	1.400
Na	mg/l	204.100	622.600	348.900	103.800	1.400	0.700
K	mg/l	12.200	22.500	16.600	2.900	-0.200	0.800
Ca	mg/l	372.300	472.000	417.800	28.600	-0.400	0.400
Mg	mg/l	105.200	154.000	126.800	14.100	-0.500	0.300
Li	mg/l	0.400	2.000	0.800	0.600	0.300	1.400
Br	mg/l	1.200	6.600	2.700	1.600	1.700	1.700

Ben Brahim et al. 2014). These studies focus mainly on geothermal potential and its applications. In this study, we focus on factors controlling groundwater mineralization. The chemical composition of groundwater is related to the solid product of rock weathering and changes with respect to time and space. Therefore, the variation on the concentration levels of the different hydrogeochemical constituents dissolved in water determines its usefulness for domestic, industrial, and agricultural purposes (Agoubi et al. 2013).

Table 2 shows that TDS ranges from 2.12 to 3.29 g/l with a mean of 2.5 g/l indicating brackish water. Temperature ranges from 43 to 65 °C indicating a contrast of temperature between deep and superficial water. Skewness ranges from -0.5 to 1.4 suggesting a Gaussian distribution for all analyzed data.

The pie diagram (Fig. 3) shows that for both superficial and deep waters, the dominant cations are Ca and Na; however, SO₄ and Cl were the dominant anions. The abundance of Na-Cl-Ca-SO₄ in groundwater is probably due to the leaching of evaporitic minerals, such as gypsum and halite. Piper diagram (Fig. 4) reveals that the dominant water type is Ca-SO₄-Na-Cl-Mg, suggesting dissolution of evaporitic minerals. The Na-

Mg-Ca-SO₄-Cl water type characterizes the lower Cretaceous aquifer (Continental Intercalary); however, the Senonian aquifer (Superficial aquifer) is Na-Cl-Ca-SO₄ water type (Bouri et al. 2008; Sahli et al. 2013). The presence of Mg in groundwater suggests that the dissolution of dolomite is the main source of magnesium in thermal ground water.

Diagram Cl vs. T and SO₄ vs. T (Fig. 5a, b) show that three water types are identified in the study area. The first type is characterized by a temperature ranging from 40 to 45 °C and Cl concentration from 500 to 900 mg/l, and SO₄ concentration values ranging from 650 to 850 mg/l represent shallow water. The second water type shows a temperature from 45 to 60 °C and low chloride concentration suggesting the mixed water (shallow and deep waters). However, the third type represents the deep water in which the temperature is above 60 °C and Cl and SO₄ concentrations ranging from 600 to 1000 mg/l.

Correlations between Na/Cl and Ca/SO₄ were tested. A diagram Na vs. Cl (Fig. 6a) shows a high correlation ($R^2 = 0.86$) between Na and Cl in the thermal water indicating that Na and Cl involve together and the two ions have a same origin, probably due to halite dissolution. Figure 6b, SO₄ vs.

Fig. 3 Pie diagram of median values of major ions

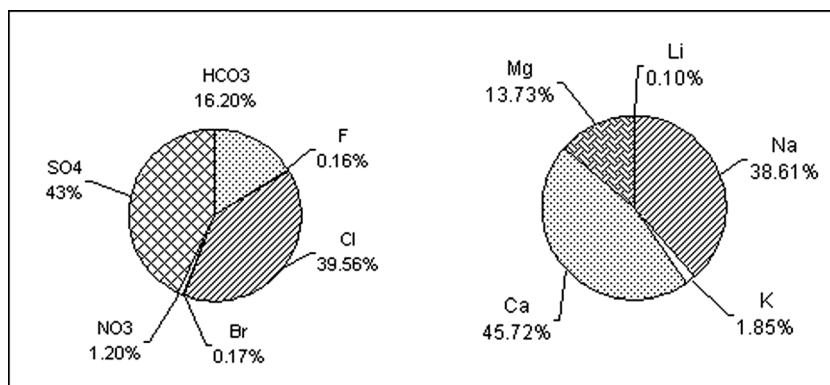
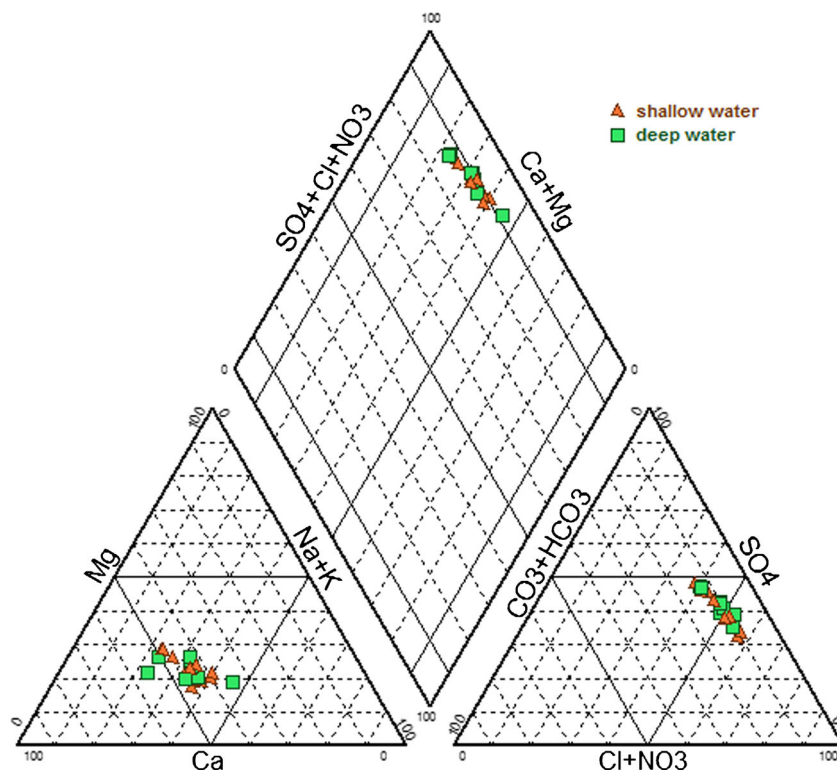


Fig. 4 Piper diagram of groundwater from the study area



Ca, shows no correlation between Ca and SO_4 and an excess of sulfate, indicating that SO_4 concentration due to gypsum dissolution and other chemical processes.

Radon-222 activity in El Hamma aquifer system

For each site, three measurements of radon-222 were taken and then averaged. The measurement and averaged radon-222 values and summary statistics are shown in Table 3. Radon concentration results changed between 203 and 2930 Bq/m^3 with a mean of 1220 Bq/m^3 . This radon concentration is comparable to the variations reported from recently published studies (Table 4). The ^{222}Rn concentration in EL Hamma thermal water is lower than thermal baths of Bursa, Turkey (Gurler et al. 2010), Island of Ikaria, Greece (Trabidou and Florou 2010), and El Castaño and Las Trincheras, Venezuela (Horvath et al. 2000), and Hot springs in Jordany (Al-Kazwini and Hasan 2003). Nevertheless, ^{222}Rn in the studied area is higher than Transylvania, Romania (Cosma et al. 2008), and Bad Gastein, Austria (Pohl-Ruling and Hofman 2002). Radon activities in the touristic city of Sarein in Iran (Jalili-Majreshin et al. 2012) are comparable with radon concentration measured in El Hamma thermal groundwater.

Radon behavior is basically determined by physical processes and not by the chemical interactions (Roba et al. 2010). Figure 7, depicting the relationship between radon and Na, K, Ca, and Mg, shows no significant correlation between radon

and major ions in thermal water. Nevertheless, radon concentration in thermal water of El Hamma seems to decrease as the temperature increases (Fig. 8) showing a high radon concentration in superficial aquifer. Figure 9 indicates that Rn-222 was anticorrelated with electrical conductivity (EC) of groundwater. It is shown in Fig. 9 that wells pumping deep aquifer (continental intercalary) (wells number 6, 7, 8, 8, 9, 10, 11, 13, and 17) have a low radon concentration ranging from 203 to 1100 Bq/m^3 and from 677 to 2903 Bq/m^3 in superficial aquifer (Table 3).

Statistical and variographic analysis

Hierarchical clustering analysis (HCA) is the most common approach in which clusters are formed sequentially, by starting with the most similar pair of objects and forming higher clusters step by step (Singh et al. 2009; Banoeng-Yakubo et al. 2008). HCA uncovers intrinsic structure of dataset, without making a priori assumption about the data, in order to classify the objects of the system into categories or clusters based on their nearness or similarity (Vega et al. 1998). HCA was applied to thermal water aquifer dataset in order to categorize the different water samples. The dendrogram of groundwater quality data from the Q-mode HCA was plotted based on Euclidean distance (Fig. 10).

Dendrogram from the Q-mode HCA based on physical parameters and major ions of groundwater (Fig. 10a)

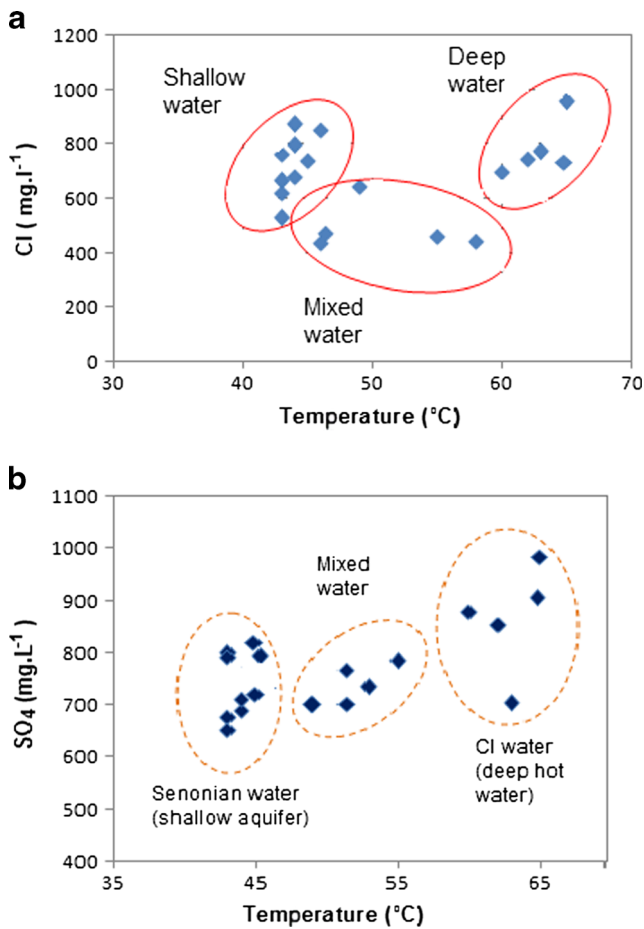


Fig. 5 Relationship between Cl, SO₄, and T in geothermal water of El Hamma, **a** Cl vs. T and **b** SO₄ vs. T

shows two clusters. The first represents the water salinity in which all parameters and major ions were clustered together. The second cluster contains only radon. These findings indicate that the radon activity was not controlled by chemical water composition. It is shown in Fig. 10b that water samples are clustered in three groups according to geochemical analysis.

Using temperature as a tracer of groundwater discharge has been the subject of several recent studies (Hunt et al. 1996; Constantz 1998; Townley and Trefry 2000; Becker et al. 2004; Hatch et al. 2010; Gerech et al. 2011). Heat has merit over chemical tracers, the temperature signature is natural, and its measurement is quick and ready to construe. (Stonestrom and Constantz 2003). Becker et al. (2004) indicate that use of temperature for estimating groundwater discharge is important in describing subsurface flow and can be useful in calibrating numerical groundwater models. Bianchin et al. (2010) used temperature measurements coupled with hydraulic head to investigate groundwater-surface water interaction.

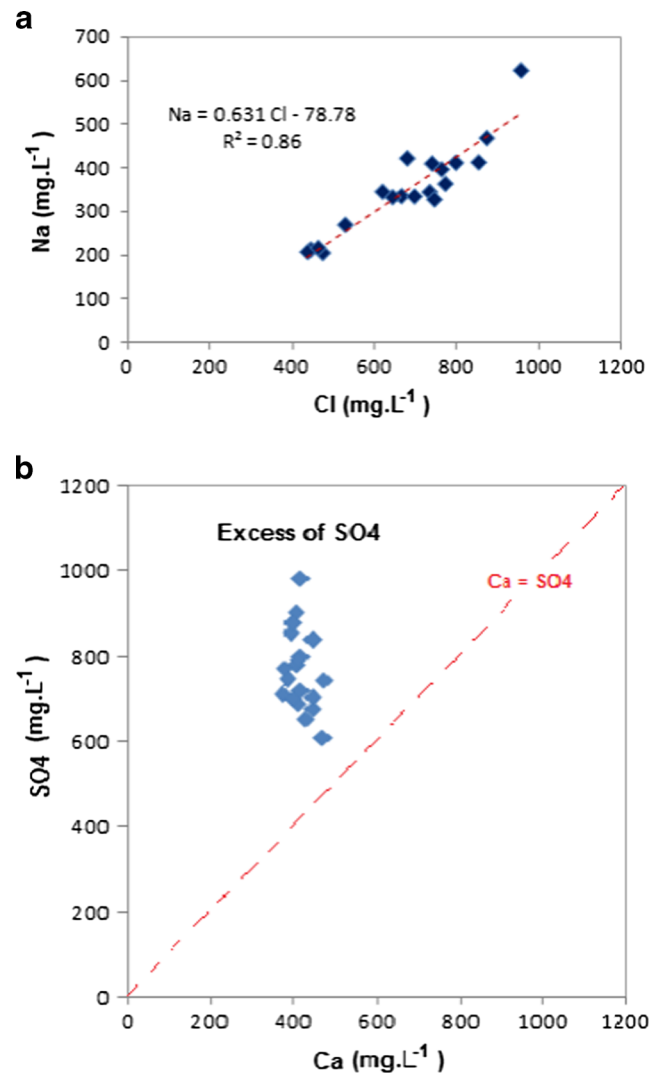


Fig. 6 Correlation between **a** Na-Cl and **b** Ca-SO₄

In order to study spatial variation of groundwater temperature and understand the communication between deep and superficial aquifers, geostatistical analysis was performed. Experimental semivariogram of temperature was computed, and several models were tested. Root mean squared error (RMSE) was used to select the best fit model.

Variographic and kriging analysis of spatial development of temperature

Geostatistical analysis was performed using EasyKrig MATLAB toolbox (Chu and Hole 2004). The EasyKrig program package uses a graphical user interface (GUI) to simplify the operation, and it works in the MATLAB environment. A specific advantage of this software is its capability to automatically generate the required default parameters, overcoming the user need to estimate initial parameter value.

Table 3 Rn-222 measurement and averaged values from wells and thermal baths of El Hamma

Sample ID	Aquifer	Rn-222 measurement ID no.			Rn-222 mean value (Bq/m ³)	Standard deviation
		#1	#2	#3		
1	SA	2090 ± 32	2075 ± 56	2135 ± 74	2100	31
2	SA	561 ± 9	768 ± 48	714 ± 69	681	107
3	SA	1213 ± 19	1225 ± 87	1252 ± 78	1230	20
4	SA	792 ± 23	817 ± 56	842 ± 29	817	25
5	SA	1514 ± 47	1546 ± 89	1620 ± 74	1560	54
6	CI	1098 ± 36	1044 ± 71	1158 ± 28	1100	57
7	CI	230 ± 12	237 ± 23	244 ± 14	237	7
8	CI	647 ± 13	663 ± 28	631 ± 36	647	16
9	CI	214 ± 8	203 ± 12	192 ± 11	203	11
10	CI	632 ± 10	613 ± 52	645 ± 27	630	16
11	CI	564 ± 14	512 ± 71	604 ± 25	560	46
12	SA	1278 ± 23	1250 ± 25	1312 ± 41	1280	31
13	CI	910 ± 24	1120 ± 23	925 ± 48	985	117
14	SA	1850 ± 28	1870 ± 87	1830 ± 56	1850	20
15	SA	660 ± 24	692 ± 26	679 ± 42	677	16
16	SA	2410 ± 84	2310 ± 47	2420 ± 85	2380	61
17	CI	643 ± 23	536 ± 26	621 ± 25	600	57
18	SA	2880 ± 89	2930 ± 58	2980 ± 77	2930	50
19	SA	2700 ± 76	2720 ± 78	2740 ± 89	2720	20
					Min	203
					Max	2930
					Mean	1220.37

SA Senonian aquifer (superficial groundwater), CI Continental intercalaire (deep groundwater)

The experimental variogram is the key of any geostatistical analysis as it helps to highlight the spatial correlations between variables. The experimental variogram is computed using the equation shown in Eq. (1).

$$\gamma(h) = \frac{1}{2N(h)} \sum_{i=1}^N [T(x_i) - T(x_i + h)]^2 \tag{1}$$

where $\gamma(h)$ is the estimated value of the semivariance for lag h , $N(h)$ is the number of experimental pairs separated by

vector h , and $T(x_i)$ and $T(x_i + h)$ are values of the variable T at x_i and $x_i + h$ locations, respectively.

Variogram of groundwater temperature (Fig. 11) is modeled Gaussian-cosine (sill = 1, range = 0.95, nugget = 0). In order to assess the model performance, double kriging cross-validation method is employed. Cross-validation is a statistical technique consisting in the partitioning of data into subsets such that the analysis is initially performed on a single subset.

Table 4 Activity concentrations of ²²²Rn in thermal waters from recent studies in the world

Country	Locality	T (°C)	Range ²²² radon (Bq/m ³)	Reference
Turkey	Thermal baths of Bursa	37–45	2513–82,553	Gurler et al. (2010)
	Denizli Basin	35–95	670–25,900	Erees et al. (2007)
Iran	Touristic city of Sarein	15–58	212–3890	Jalili-Majareshein et al. (2012)
Greece	Island of Ikaria	45–65	100–57,600	Trabidou and Florou (2010)
Romania	Transylvania	NA	0.5–129.3	Cosma et al. (2008)
Venezuela	El Castaño and Las Trincheras	NA	1000–560,000	Horvath et al. (2000)
Jordany	Hot springs (many locations)	NA	63,000–81,000	Al-Kazwini and Hasan (2003)
Tunisia	Thermal water of El Hamma	43–65	203–2930	This study

NA not available

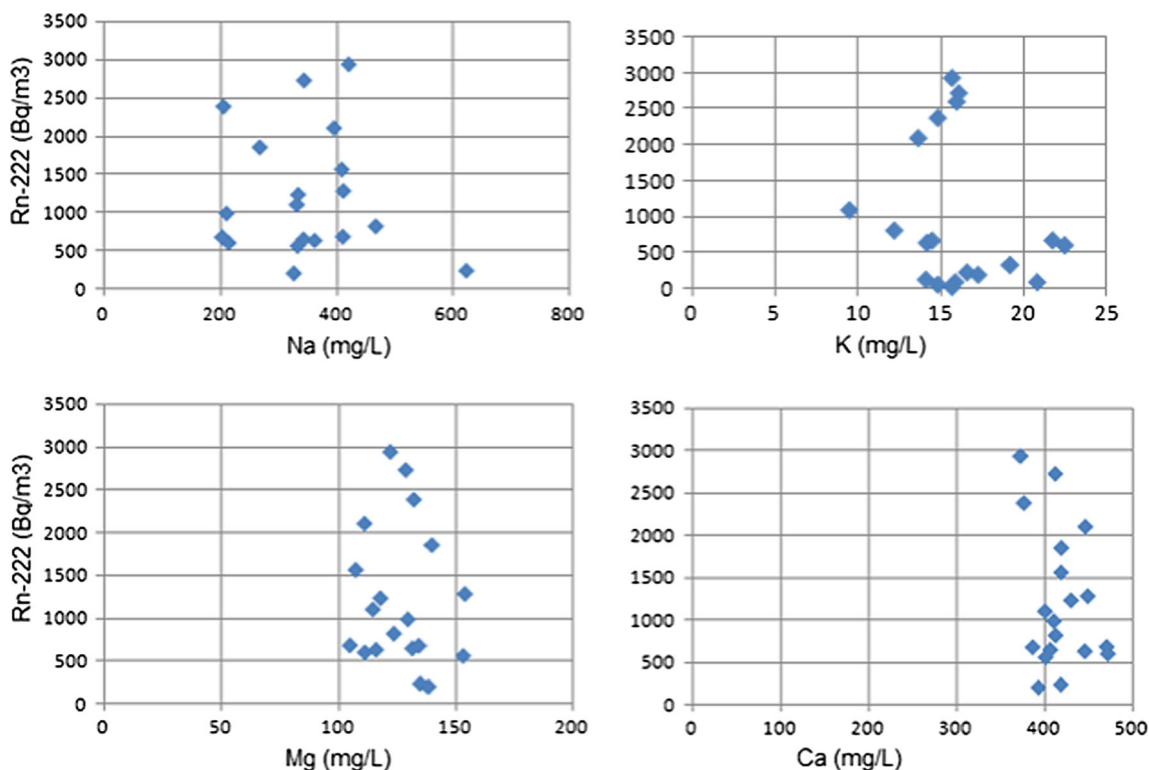


Fig. 7 Radon-222 vs. Na, Mg, K, and Ca concentration from the study area

Subsequently, the other subsets are used in confirming the initial analysis.

The double kriging cross-validation scheme is used to evaluate the level of agreement between the kriged or predicted values and the original observations at all observation locations. The predicted data at grids obtained from the kriging (first stage) are served as “input data.” The mean value at the original observation locations are estimated by kriging (second stage) with the same kriging

parameters and variogram model parameters. The results from the second kriging are then compared with the original observed data in a separate plot (Chu and Hole 2004; Di Piazza et al. 2009).

Double kriging cross-validation between observed and predicted values of groundwater temperature is shown in Fig. 12. We notice very good matching between observed and estimated data that confirms the selection of Gaussian-cosine model that is very suitable

Fig. 8 Relationship between radon and temperature

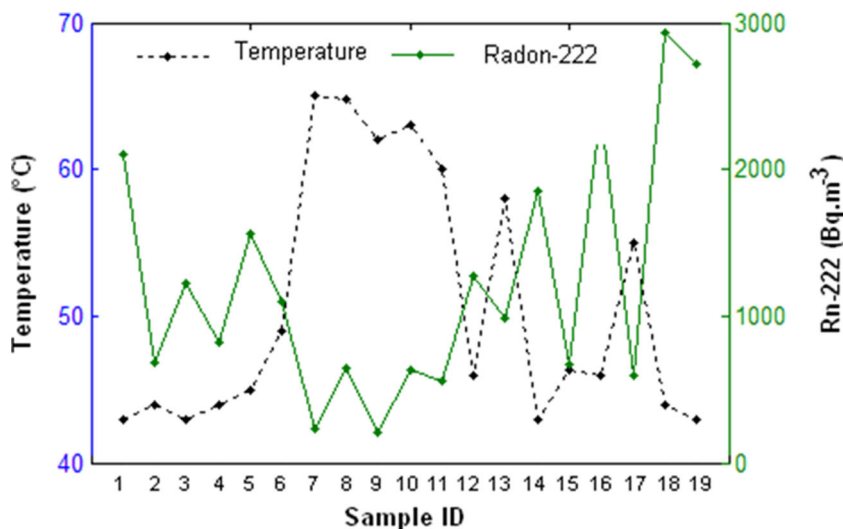


Fig. 9 Relationships between Rn-222 and EC

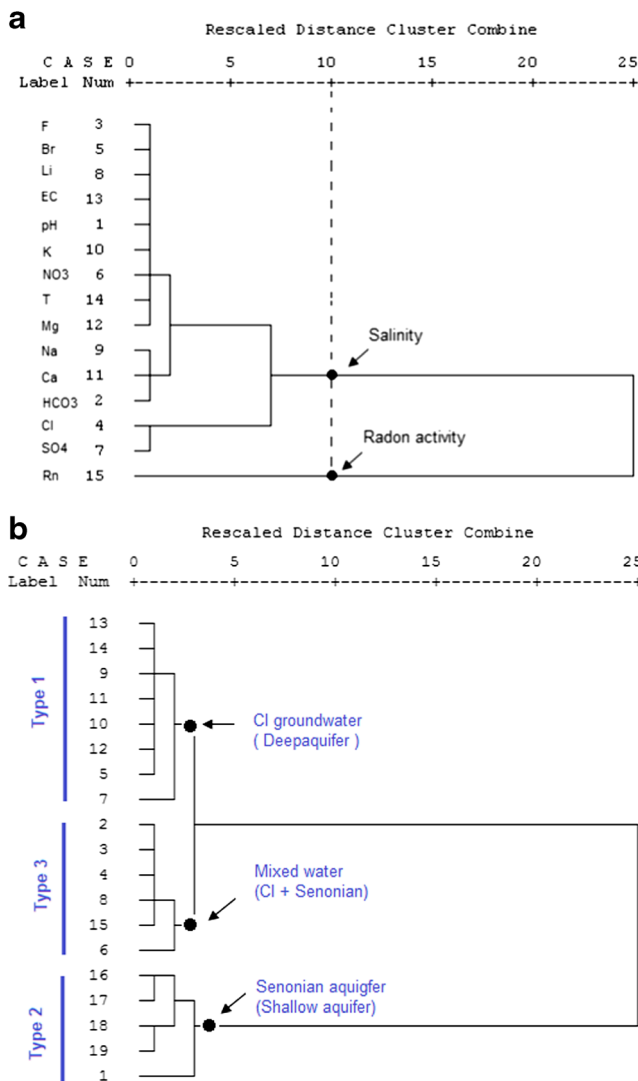
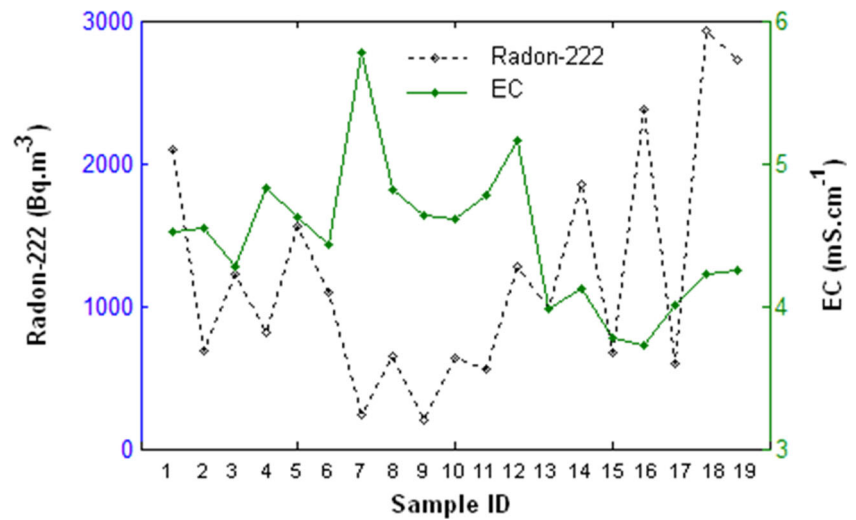


Fig. 10 Dendrogram of thermal waters from the Q-mode HCA including all water samples. **a** The cluster analysis is based on the major ion parameters; **b** cluster is based on sampled waters (well and bath)

for modeling the spatial variability of groundwater temperature.

RMSE is also used to test the model performance. This parameter is often used to compare the

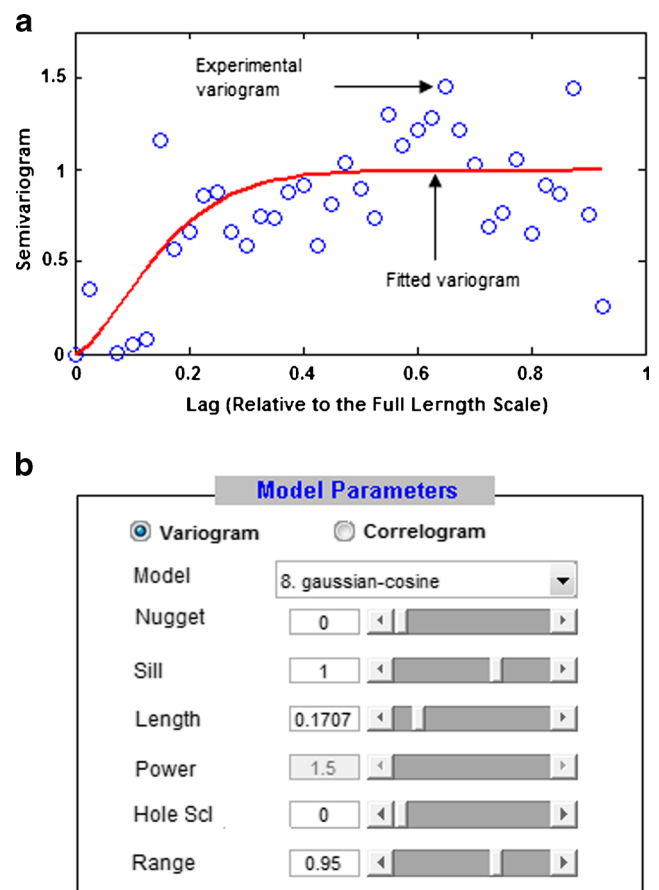


Fig. 11 Variogram analysis of groundwater temperature. **a** Experimental and fitted variogram (blue circle experimental variogram, red line fitted model); **b** model parameters

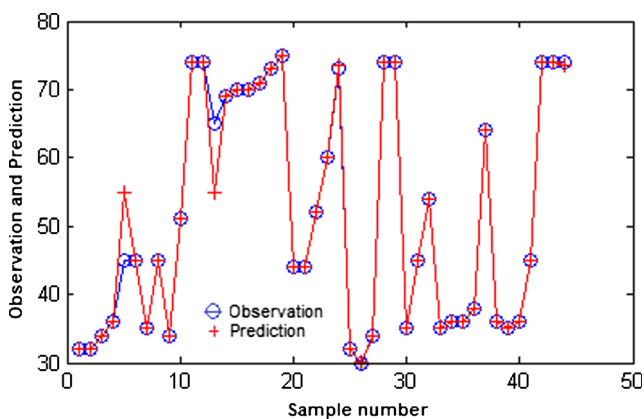


Fig. 12 Double kriging cross-validation between observed and predicted values

performance of interpolation methods. RMSE is computed according to Eq. (2):

$$RMSE = \sqrt{\frac{1}{n} \sum_{i=1}^n [T(x_i) - T^*(x_i)]^2} \quad (2)$$

where $T(x_i)$ is the observed value and $T^*(x_i)$ corresponds to the predicted value of observation i in location x_i . The smallest value of RMSE is considered as the best fitted one. The RMSE computed for Gaussian-cosine model is 0.02 with a standard deviation $\sigma = 2.159$.

Spatial vertical variation of groundwater temperature of El Hamma aquifer system (Fig. 13) was developed based on ordinary kriging. Based on previous results, water temperature in the saturated area of aquifer system is controlled by geology. Figure 13 shows that the vertical high temperature in vertical faults is comparable with CI temperature. This temperature is the same nearby the faults, suggesting a vertical flow of groundwater from Continental Intercalary (deep aquifer) to superficial Senonian aquifer. Groundwater ascension is controlled by hydrodynamic parameters of CI. CI water table is higher than Senonian piezometric level allowing the vertical ascension of groundwater to superficial aquifer.

Hydrogeological conceptual model and radon emanation

Groundwater of deep aquifer display significantly lowers ^{222}Rn activities than shallow groundwater in study area. The difference between the activities of radon deep aquifer and the water surface was controlled by lithology and petrophysical characteristics of the rock matrix. The radon anomalies show characteristic features which may be structurally controlled (King et al. 1996; Gainon et al. 2007). Thus, CI aquifer comprises sandstone (less than 10 % clay) clay and sandstones (10 to 50 % clay) (ERESS 1972). The porosity of the aquifer is between 22.6 and 28.7 % (ERESS 1972).

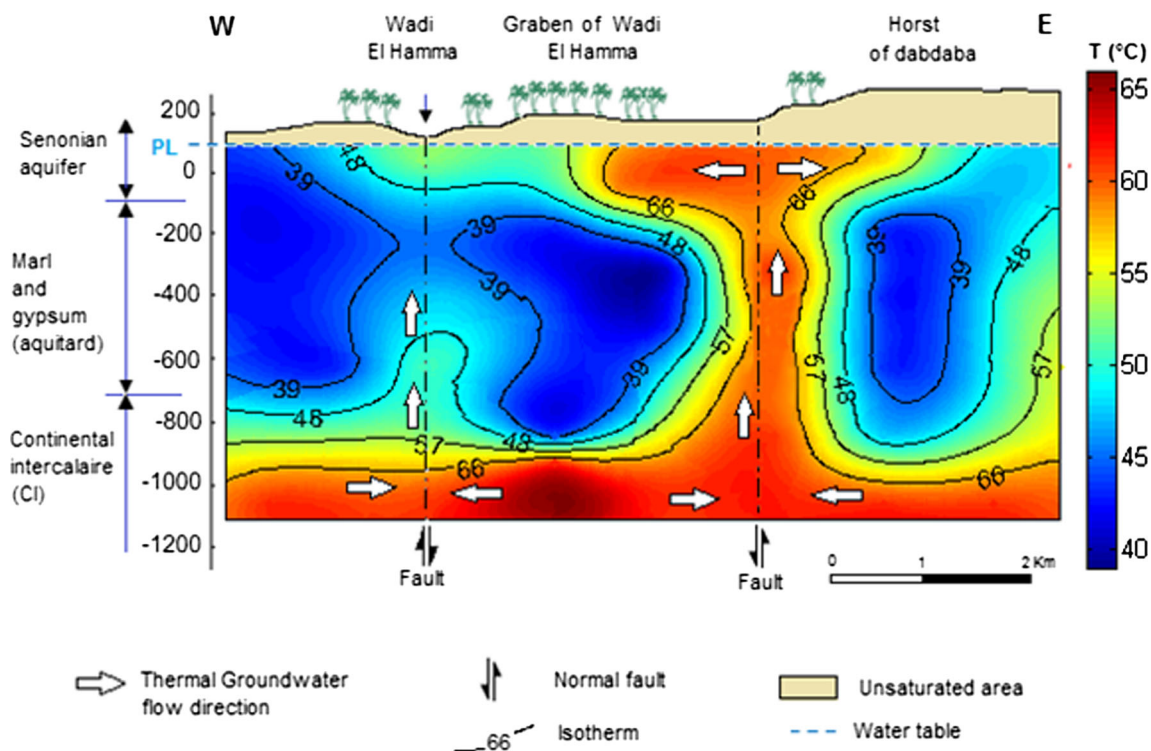
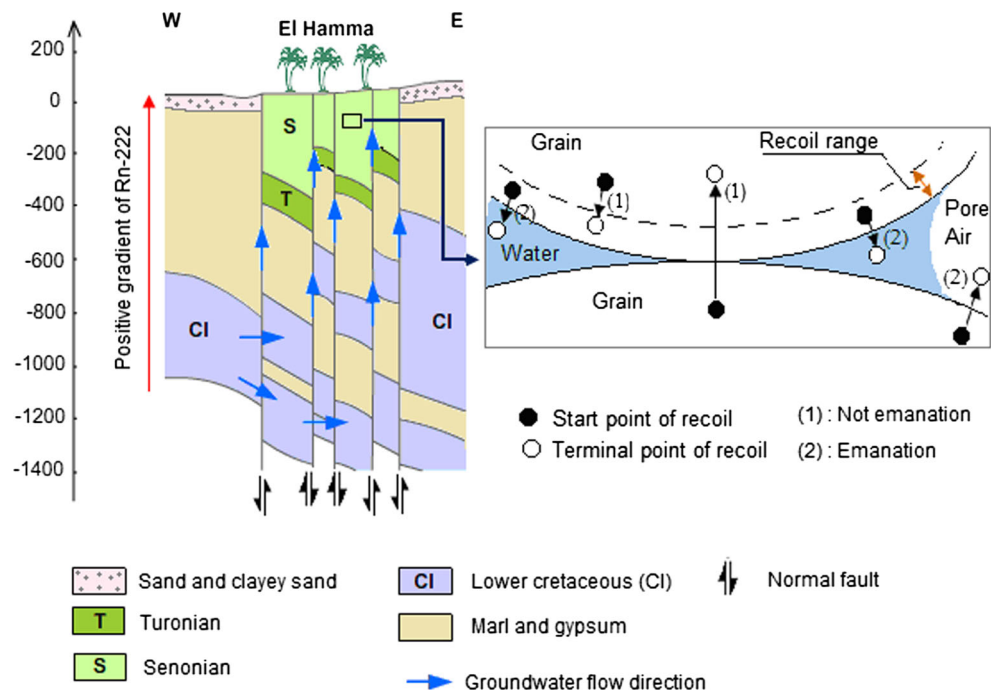


Fig. 13 Krigged model of thermal groundwater flow via fault system

Fig. 14 Hydrogeological conceptual model of groundwater flow system (after Abidi 2004, modified) and radon-222 emanation phenomenon (after Ferry et al. 2001)



Groundwater often flows through rocks containing natural uranium, and radium produces radon gas that dissolves easily in water. That is why water from wells dug normally has much higher radon than surface water in rivers, lakes, or streams. Higher radon concentration values are, in general, found to be associated with springs that are controlled by faults. Thus, the radon contents in spring samples are found to be highly variable in accordance with its genetic type and depth of groundwater circulation (Choubey et al. 2007).

The factor of emanation of a porous medium is dependent on the nature of the solid matrix, particle size, pore size, and distribution of radium in the grain. Figure 14 shows that ^{226}Ra atom (black grains) emanates directly in water or in air contained in the pores. However, if the grains of radium are trapped in the solid matrix in which they are formed or are trapped in neighboring grains, then there will be no emanation.

Deep water circulation was controlled by geology and hydrodynamic characteristics of aquifer system. Based on the geological features and the interpretation of chemical and isotopic fluid geochemistry, Bouri et al. (2008) has indicated that southeast Tunisia thermal springs, particularly in Zarat region, are fed by mixtures of Senonian and lower Cretaceous waters in varying proportions.

The lower cretaceous (CI) water table was higher than piezometric surface of Senonian aquifer in El Hamma region (Bouri et al. 2008). A hydrodynamic pressure applied to lower cretaceous water during the deep water circulation. The water flow direction is in the direction of open fractures, faults, and karstic. According to Fig. 14, hot deep waters ascend through

fractures and faults and mix with Senonian waters. The Neogene formations are relatively impermeable and cap the system.

Conclusions

Geochemical composition, radon concentration, and temperature measurement of geothermal groundwater from wells and bath in El Hamma City were carried out in order to study groundwater chemistry and its flow direction in El Hamma aquifer system. The results presented above demonstrate that geothermal groundwater chemistry was controlled by lithology and rock-water interaction. Hot temperature of geothermal groundwater from shallow and deep aquifer activates a chemical processes of rock-water interaction and dissolution of halite (NaCl), calcite (CaCO_3), gypsum (CaSO_4), and dolomite ($\text{CaMg}(\text{CO}_3)_2$).

Based on geochemical composition, three groups of water salinity were found in El Hamma aquifer system: deep hot groundwater, shallow water, and mixed groundwater. The relations between major ions strongly confirm the mixing process. The dominant water facies was $\text{Ca-SO}_4\text{-Na-Cl-Mg}$.

The observed concentration of radon both in shallow and deep aquifer reveals that ^{222}Rn activity is higher in the shallow aquifer. These activities associated different fault and thrust that help in the easy escape of radon from shallow aquifer. It has been also noticed that the ^{222}Rn emanation was controlled by geology, permeability, and porosity of Senonian calcareous

aquifer. Thus, the radon concentration measurement in thermal baths and dug wells may be useful in discriminating deep water, mixed water, and shallow aquifer influenced by rainfall.

Temperature, used as tracer of geothermal groundwater flow, indicates a vertical flow from continental intercalary to shallow aquifer via vertical fault system. These faults facilitate the ascension of deep heat water to superficial aquifer.

Acknowledgments This work was conducted at the Higher Institute of Water Sciences and Techniques, University of Gabes. The authors would like to thank Prof. Younes Jedoui (UR-HSA) for the help in financing the research works and performing geochemical analysis in the research laboratory of geochemical and isotopic analysis.

References

- Abidi B (2004) Caractéristique hydrodynamique et géochimique de la djefara de gabès, DRE de Gabès; 120 p (in french)
- Agoubi B, Kharroubi A, Abida H (2013) Hydrochemistry of groundwater and its assessment for irrigation purpose in coastal Jeffara Aquifer, southeastern Tunisia. *Arab Journal Geosciences* 6:1163–1172. doi:10.1007/s12517-011-0409-1
- Akawwi E (2014) Radon-222 concentration in the groundwater along eastern Jordan rift. *J Appl Sci* 14(4):309–316. doi:10.3923/jas.2014.309.316
- Al-Kazwini AT, Hasan MA (2003) Radon concentration in Jordanian drinking water and hot springs. *J Radiol Prot* 23:439. doi:10.1088/0952-4746/23/4/007
- Banoeng-Yakubo B, Mark Yidana S, Nti E (2008) Hydrochemical analysis of groundwater using multivariate statistical methods—the Volta Region, Ghana. *KSCE J Civ Eng* 13:55–63
- Becker MW, Georgian T, Ambrose H, Siniscalchi J, Fredrick K (2004) Estimating flow and flux of groundwater discharge using water temperature and velocity. *J Hydrol* 296(1–4):221–233
- Ben Brahim F, Makni J, Bouri S, Ben Dhia H (2014) Evaluation of temperature and mixing process of water in deep and shallow aquifers in the southwestern Tunisia: case of Djerid Region. *Arab J Sci Eng*. doi:10.1007/s13369-014-1138-z
- Ben Oueddou H (1984) Stratigraphy of quaternary continental deposits around the Gulf of Gabès (Southern Tunisia). *Comptes-rendus des séances de l'Académie des sciences, Mécanique-physique, chimie, sciences de l'univers, sciences de la terre. Série II* 299(19):1351–1354
- Bianchin M, Smith L, Beckie R (2010) Quantifying hyporheic exchange in a tidal river temperature times series, water. *Resour Res* 46:W97507. doi:10.1029/2009WR008365
- Bouri S, Makni J, Ben Dhia H (2008) Synthetic approach integrating surface and subsurface data for prospecting deep aquifers: the southeast Tunisia. *Environ Geol* 54:1473–1484. doi:10.1007/s00254-007-0928-y
- Bravo HR, Fen J, Hunt RJ (2002) Using groundwater temperature data to constrain parameter estimation in a groundwater flow model of a wetland system. *Water Resour Res* 38(8) doi:10.1029/2000WR000172
- Castany G (1982) Bassin sédimentaire du Sahara septentrional (Algérie-Tunisie). *Aquifères du Continental Intercalaire et du Complexe Terminal. Bull Bur Rech Géol Min (BRGM) Sér. 2* 3:127–147
- Choubey VM, Mukherjee PK, Bajwa BS, Walia V (2007) Geological and tectonic influence on water–soil–radon relationship in Mandi-Manali area, Himachal Himalaya. *Environ Geol* 52:1163–1171. doi:10.1007/s00254-006-0553-1
- Chu D, Hole W (2004) The GLOBEC kriging software package—EasyKrig3.0
- Constantz J (1998) Interaction between stream temperature, stream flow and groundwater exchanges in alpine streams. *Water Resour Res* 36(7):1609–1616
- Cosma C, Moldovana M, Dicua T, Kovacs T (2008) Radon in water from Transylvania (Romania). *Radiat Meas* 43:1423–1428
- Di Piazza A, Di Piazza MC, Vitale G (2009) A kriging-based partial shading analysis in a large photovoltaic field for energy forecast. *International Conference on Renewable Energies and Power Quality (ICREPQ'09) Valencia (Spain)*
- Durrige Company Inc. (2000) RAD7 radon detector. In: User manual (ver. 7.0), Bedford, MA, United States
- Edmunds WM, Guendouz AH, Mamou A, Moulla A (2003) Groundwater evolution in the Continental intercalaire aquifer of south Algeria and Tunisia: trace element and isotopic indicators. *Appl Geochem* 18:805–808
- El-Fiky A (2009) Hydrogeochemistry and geothermometry of thermal groundwater from the Gulf of Suez Region, Egypt. *JKAU Earth Sci* 20(2):71–96
- Erees FS, Aytas S, Sac MM, Yener G, Salk M (2007) Radon concentrations in thermal waters related to seismic events along faults in the Denizli Basin, Western Turkey. *Radiat Meas* 42:80–86
- ERESS (1972) Nappe de la zone côtière du sud tunisien (djefara), modèle analogique. *Programme des Nations unies, UNESCO, vol 4*
- Ferry C, Richon P, Beneito A, Robé MC (2001) Radon exhalation from uranium milltailings: experimental validation of a 1-D model. *J Environ Radioact* 54:99–108
- Gainon F, Goldscheider N, Surbeck H (2007) Conceptual model for the origin of high radon levels in spring waters the example of the St. Placidus spring, Grisons, Swiss Alps. *Swiss J Geosci* 100:251–262. doi:10.1007/s00015-007-1220-6
- Gerecht KE, Cardenas MB, Guswa AJ, Sawyer AH, Nowinski JD, Swanson TE (2011) Dynamics of hyporheic flow and heat transport across a bed-to-bank continuum in a large regulated river. *Water Resour Res* 47:W03524. doi:10.1029/2010WR009794
- Gokhale B, Leung S (2010) Groundwater radon-222 concentrations in Antelope Creek, Idaho: measurement and interpolation. *Environ Biol Monit J* 3:12–20
- Gurler O, Akar U, Kahraman A, Yalcin S, Kaynak G, Gundogdu O (2010) Measurements of radon level in thermal waters of Bursa, Turkey. *Fresenius Environ Bull* V19-12a:3013–3017
- Hatch CE, Fisher AT, Ruehland C, Stemler G (2010) Spatial and temporal variations in streambed hydraulic conductivity quantified with time-series thermal methods. *J Hydrol* 389:276–288
- Horvath A, Bohus LO, Urbani F, Marx G, Piroth A (2000) Radon concentrations in hot spring waters in northern Venezuela. *J Environ Radioact* 47:127–133
- Hunt MW, Georgian T, Ambrose H, Siniscalchi J, Fredrick K (1996) Groundwater inflow measurements in wetland systems. *Water Resour Res* 32(3):495–508
- Jalili-Majrareshin A, Behtash A, Rezaei-Ochbelagh D (2012) Radon concentration in hot springs of the touristic city of Sarein and methods to reduce radon in water. *Radiat Phys Chem* 81:749–757
- Kendall C, McDonnell JJ (1998) *Isotopes tracers in catchment hydrology*. Elsevier Science B.V, Amsterdam
- King CY, King BS, Evans WC, Zhang W (1996) Spatial radon anomalies on active faults in California. *Appl Geochem* 11:497–510
- Louhaichi MA, Tlig S (1993) Tectonique synsédimentaire des séries crétacées post-barrémiennes au Nord de la chaîne des chotts (tunisie méridionale). *Géol Méditer*, Tome XX, n° 1, p 53-74
- Nikolopoulos D, Vogianis E, Louizi A (2009) Radon concentration of waters in Greece and Cyprus. *Geophys Res Abstr* 11:EGU2009–EGU3786 2009
- Pohl-Ruling J, Hofman W (2002) Investigation of cancer mortality in the Gastein Valley, an area of high-level natural radiation. *Int Congr Ser* 1236:27–29

- Roba CA, Codrea V, Moldovan M, Baciuc C, Cosma C (2010) Radon and radium content of some cold and thermal aquifers from Bihor County (northwestern Romania). *Geofluids* 10:571–585. doi:10.1111/j.1468-8123.2010.00316.x
- Sahli H, Tagorti MA, Tlig S (2013) Groundwater hydrochemistry and mass transfer in stratified aquifer system (Jeffara Gabes basin, Tunisia). *Larhyss J* 12:95–108
- Senior LA (1998) Radon-222 in the ground water of Chester County, Pennsylvania. U.S. Department of the Interior, U.S. Geological Survey, Water-Resources Investigations Report 98–4169
- Singh AK, Mondal GC, Tewary BK, Sinha A (2009) Major ion chemistry, solute acquisition process and quality assessment of mine water in Damodar valley coalfields, India. Abstracts of the International Mine Water Conference, 19th – 23rd October 2009, Pretoria, South Africa
- Stonestrom DA, Constantz J (2003) Heat as a tool for studying the movement of groundwater near streams, USGS Circ 1260
- Townley LR, Trefry MG (2000) Surface water-groundwater interaction near shallow circular lakes: flow geometry in three dimensions. *Water Resour Res* 36(4):935–949
- Trabelsi R, Kacem A, Zouari K (2009) Rozanski K (2009) quantifying regional groundwater flow between Continental intercalaire and Djeffara aquifers in southern Tunisia using isotope methods. *Environ Geol* 58:171–183. doi:10.1007/s00254-008-1503-x
- Trabidou G, Florou H (2010) Estimation of dose rates to humans exposed to elevated natural radioactivity through different pathways in the Island of Ikaria, Greece. *Radiat Prot Dosim* (2010) 142(2–4):378–384
- USEPA (1999) U.S. Environmental Protection Agency. National primary drinking water regulations, radon-222. *Federal Register*: November 2, 1999; 64 (211)
- USEPA (2008) U.S. Environmental Protection Agency. Radon. <http://www.epa.gov/radon/>. Accessed 31 Jan 2014
- Vega M, Pardo R, Barrado E, Deban L (1998) Assessment of seasonal and polluting effects on the quality of river water by exploratory data analysis. *Water Res* 32:3581–3592
- Voronov AN (2004) Radon-rich waters in Russia. *Environ Geol* 46:630–634. doi:10.1007/s00254-003-0857-3
- Wu Y, Wen X, Zhang Y (2003) Analysis of the exchange of groundwater and river water by using radon-222 in the middle Heihe Basin of north-western China. *Environ Geol* 45:647–653